Cellular/Molecular

Molecular Determinants of KCNQ (K_v7) K^+ Channel Sensitivity to the Anticonvulsant Retigabine

Anne Schenzer,[1]* Thomas Friedrich,[2]* Michael Pusch,[3] Paul Saftig,[1] Thomas J. Jentsch,[4] Joachim Grötzinger,[1] and Michael Schwake[1]

[1]Institute of Biochemistry, Christian-Albrechts-University Kiel, D-24098 Kiel, Germany, [2]Max-Planck-Institute of Biophysics, D-60438 Frankfurt/Main, Germany, [3]Istituto di Biofisica, I-16149 Genova, Italy, and [4]Zentrum für Molekulare Neurobiologie Hamburg, D-20251 Hamburg, Germany

Epilepsy is caused by an electrical hyperexcitability in the CNS. Because K^+ channels are critical for establishing and stabilizing the resting potential of neurons, a loss of K^+ channels could support neuronal hyperexcitability. Indeed, benign familial neonatal convulsions, an autosomal dominant epilepsy of infancy, is caused by mutations in *KCNQ2* or *KCNQ3* K^+ channel genes. Because these channels contribute to the native muscarinic-sensitive K^+ current (M current) that regulates excitability of numerous types of neurons, KCNQ (K_v7) channel activators would be effective in epilepsy treatment. A compound exhibiting anticonvulsant activity in animal seizure models is retigabine. It specifically acts on the neuronally expressed KCNQ2–KCNQ5 ($K_v7.2$–$K_v7.5$) channels, whereas KCNQ1 ($K_v7.1$) is not affected. Using the differential sensitivity of KCNQ3 and KCNQ1 to retigabine, we constructed chimeras to identify minimal segments required for sensitivity to the drug. We identified a single tryptophan residue within the S5 segment of KCNQ3 and also KCNQ2, KCNQ4, and KCNQ5 as crucial for the effect of retigabine. Furthermore, heteromeric KCNQ channels comprising KCNQ2 and KCNQ1 transmembrane domains (attributable to transfer of assembly properties from KCNQ3 to KCNQ1) are retigabine insensitive. Transfer of the tryptophan into the KCNQ1 scaffold resulted in retigabine-sensitive heteromers, suggesting that the tryptophan is necessary in all KCNQ subunits forming a functional tetramer to confer drug sensitivity.

Key words: **epilepsy; KCNQ; M current; potassium channels; retigabine; excitability**

Introduction

Mutations in four of the five human *KCNQ* genes [proteins, $K_v7.1$–$K_v7.5$ (Gutman et al., 2003), here referred to as KCNQ1–KCNQ5] lead to inherited diseases (Jentsch, 2000). Dominant-negative *KCNQ1* mutations are associated with cardiac arrhythmias (Wang et al., 1996), whereas patients carrying recessive mutations on both alleles additionally suffer from congenital deafness (Neyroud et al., 1997). In contrast, a gain-of-function mutation was found in patients with an autosomal dominant atrial fibrillation (Chen et al., 2003). Mutations in *KCNQ2* or *KCNQ3* lead to dominantly inherited benign familial neonatal convulsions, a neonatal epilepsy (Biervert et al., 1998; Charlier et al., 1998; Singh et al., 1998). Mutations in *KCNQ4* underlie a form of dominant progressive hearing loss (Kubisch et al., 1999).

KCNQ2 and KCNQ3 are mainly found in the nervous system and colocalized in several neuronal populations (Schroeder et al., 1998; Cooper et al., 2000). This suggests that KCNQ2 and KCNQ3 form heteromeric channels in a subset of neurons, which is further supported by heterologous expression (Schroeder et al., 1998; Yang et al., 1998) and coimmunoprecipitation studies (Cooper et al., 2000). However, both proteins are not always colocalized in brain (Cooper et al., 2000). It is thus likely that, within the CNS, also homo-oligomeric KCNQ2 or KCNQ3 channels are expressed, which are known to be functional in heterologous expression systems (Schroeder et al., 1998; Yang et al., 1998).

KCNQ2–5, and in particular KCNQ2/3 heteromers, display properties of M-type K^+ channels (Wang et al., 1998; Kubisch et al., 1999; Schroeder et al., 2000). These channels display slowly activating and deactivating K^+ currents with distinct electrophysiological and pharmacological properties and are suppressed by the activation of muscarinic acetylcholine receptors (Brown and Adams, 1980). Because M-type K^+ channels are already active at slightly depolarized potentials around the threshold of action potential firing, their modulation may control neuronal excitability. This suggests that activators of KCNQ2/3 channels might be useful in treating epilepsy. Indeed, after the identification of *KCNQ2* and *KCNQ3* as genes underlying a form of human epilepsy, it became clear that the anticonvulsive drug retigabine [*N*-(2-amino-4-[fluorobenzylamino]-phenyl)carbamic acid; D-23129] activates these channels (Wickenden et al., 2000).

The major effect of retigabine on KCNQ channels is a shift of their voltage dependence to hyperpolarized membrane voltages, resulting in an increase of K^+ currents close to the resting potential of neurons. In addition, retigabine accelerates the activation

Received Jan. 19, 2005; revised April 15, 2005; accepted April 15, 2005.

This work was supported by Deutsche Forschungsgemeinschaft Grants SCHW 866/3 (M.S.) and FR 1276/1 (T.F.), the Max-Planck-Society for the Advancement of Sciences, a fellowship from the Novartis Foundation for Therapeutic Research (M.S.), the Italian Research Ministry (Fondo per gli Investimenti della Ricerca di Base Grant RBAU01PJMS) (M.P.), and Telethon Italy Grant GGP04018 (M.P.). We thank Katharina Stiebeling for technical assistance. We are grateful to Dr. Christiane Kronbach from Elbion AG (Radebeul, Germany) for discussions and retigabine supply, and we thank Ernst Bamberg for personal and scientific support.

*A.S. and T.F. contributed equally to this work.

Correspondence should be addressed to Michael Schwake, Institute of Biochemistry, Christian-Albrechts-University Kiel, Olshausenstrasse 40, D-24098 Kiel, Germany. E-mail: mschwake@biochem.uni-kiel.de.

DOI:10.1523/JNEUROSCI.0128-05.2005

 0270-6474/05/255051-10$15.00/0

and slows the deactivation of these currents (Tatulian et al., 2001). Retigabine-treated KCNQ2/KCNQ3 channels had a more negative half-activation potential and a higher maximal open probability, which both give rise to the increase of the macroscopic current amplitudes (Tatulian and Brown, 2003). Of particular clinical importance is the fact that retigabine does not affect cardiac KCNQ1 channels but has a significant impact only on KCNQ2–KCNQ5 isoforms (Tatulian et al., 2001; Wickenden et al., 2001).

Given the physiological importance of KCNQ channels and their potential role as drug targets, we set out to identify structures determining their subunit-specific retigabine sensitivity. A chimeric approach was chosen in which distinct protein segments between KCNQ1 and KCNQ3 were exchanged, because, from all KCNQ channels, KCNQ3 exhibits the largest shift in voltage dependence in response to retigabine. We thereby identified a crucial amino acid important for the retigabine sensitivity of KCNQ K^+ channels.

Materials and Methods

cDNA constructs. Starting from KCNQ cDNAs, which were subcloned into the expression vector pTLN, the KCNQ1/KCNQ3 chimeras and point mutants were constructed by recombinant PCR and verified by sequencing. After linearization with *Hpa*I, capped RNA was transcribed using SP6 RNA polymerase in mMessage mMachine kit (Ambion, Austin, TX).

Expression in Xenopus laevis *oocytes.* Individual stage V–VI oocytes were obtained from anesthetized frogs and isolated by collagenase treatment. Total KCNQ cRNA (10 ng) was injected into oocytes (also for coinjection experiments, which contained a 1:1 cRNA mixture). After injection, oocytes were kept at 17°C in ND96 solution (in mM: 96 NaCl, 2 KCl, 1.8 $CaCl_2$, 1 $MgCl_2$, and 5 HEPES, pH 7.4).

Electrophysiology. Three to 5 d after injection, two-electrode voltage-clamp measurements were performed at room temperature in ND96 using a Turbotec05 amplifier (NPI Electronics, Tamm, Germany) and pClamp8 software (Axon Instruments, Union City, CA). For experiments examining the effect of retigabine, 10 μM retigabine was added to ND96 from a 116 mM retigabine stock solution, which was prepared in DMSO and kept at 4°C in the dark. Voltage protocols for current recordings were as follows (unless stated differently): starting from a holding potential of −80 mV, cells were clamped for 3 s (see data in Fig. 1) or 2 s (see Figs. 2–7) to test potentials between −140 and +140 mV in steps of 20 mV, followed by a 200 ms tail pulse to −30 mV. Tail current analysis was used to determine I/I_{max} curves (which are sometimes referred to as apparent p_{open} in the literature). Because the KCNQ3(S5-TD;Q1) chimera does not reach stationary current amplitudes even after 3 s, the parameters obtained for this construct do not reflect steady-state values. Tail current amplitudes were measured at −30 mV by extrapolating to the time of the voltage step. Because channel gating is slow compared with the voltage jump, these currents are proportional to the number of channels that are open at the preceding test-pulse voltage. Values were obtained from at least three different batches of oocytes with at least six oocytes per batch. The values were normalized to the mean tail current amplitude at +40 mV measured in the absence of retigabine and averaged. Values are given as means ± SEs, unless stated otherwise.

Quantitative analyses of I/I_{max} *curves and dose–response curves.* To determine the parameters for the voltage dependence of activation, I/I_{max} curves were fitted by a Boltzmann function:

$$B(V) = \frac{B_{max} - B_{min}}{1 + \exp\left(\frac{R \times T}{z_q \times F} \times (V - V_{1/2})\right)} + B_{min},$$

where B_{min} and B_{max} are the minimal or maximal I/I_{max} values, respectively, R is the molar gas constant, z_q is the slope factor (equivalent charge), F is the Faraday constant, T is the absolute temperature in kelvins, V is the transmembrane potential, and $V_{1/2}$ is the potential of half-maximal activation. Dose–response curves were fitted with a Hill equation:

$$V = V_{max} \times \frac{c^{n_H}}{K_{0.5}^{n_H} + c^{n_H}},$$

where V_{max} is the saturation value for the shift of the $V_{1/2}$ curves in response to retigabine, c is the retigabine concentration, $K_{0.5}$ is the concentration for the half-maximal $V_{1/2}$ shift, and n_H is the Hill coefficient.

Molecular modeling. Three-dimensional models for KCNQ1 and KCNQ3 were generated using the x-ray structure of KvAP (Protein Database accession number 1ORQ) as a template. The initial sequence alignment between KvAP, KCNQ1, and KCNQ3 was generated with the ClustalW program using standard parameters. In addition, a secondary structure prediction was performed for KCNQ1 and KCNQ3 to prove whether the predicted transmembrane α-helices were correctly aligned with the α-helices of the KvAP structure, leading to refinements of the initial alignment in regions of low homology. The resulting sequence alignment is shown in Figure 2. According to this alignment, amino acid residues were exchanged in the template structure (Protein Database accession number 1ORQ). Insertions and deletions in KvAP were modeled by using a database search approach included in the software package WHATIF (Vriend, 1990). The database was searched for a peptide sequence of the appropriate length, which was fitted into the template. All loops were selected from the database so as to give a minimum root mean square distance between the ends of the loops and the helices. Loops with unfavorable backbone dihedral angles or van der Waals clashes were excluded. Finally, these model structures were energy minimized, using the steepest descent algorithm implemented in the GROMOS force field (van Gunsteren et al., 1996). The structural representation was performed with the RIBBON program (Carson, 1991). All programs were run on a Silicon Graphics (Mountain View, CA) Indigo workstation.

Results

Retigabine sensitivities of KCNQ1 and KCNQ3

We first compared the effect of retigabine on KCNQ1, KCNQ2, and KCNQ3 expressed as homomers in *Xenopus* oocytes (Fig. 1). Tail current analysis was used to determine normalized I/I_{max} curves (which are sometimes referred to as apparent p_{open} curves in the literature). From a holding potential of −80 mV, oocytes were clamped for 3 s to values between −140 and +40 mV (Fig. 1*B*). Tail current amplitudes were measured in response to a voltage step to −30 mV by extrapolating to the time of the voltage step and normalized to the mean tail current amplitude at +40 mV measured in the absence of retigabine (see Materials and Methods). In line with results from mammalian cell lines (Tatulian et al., 2001), KCNQ3 (Fig. 1*C*,*E*) and KCNQ2 (Fig. 1*G*) currents were affected by 10 μM retigabine, whereas KCNQ1 was insensitive (Fig. 1*D*,*F*). The values for the voltages of half-maximal activation as determined from fitting a Boltzmann function to the I/I_{max} data (see Materials and Methods) are summarized in Table 1. Values were as follows: KCNQ1, $V_{1/2} = -29.1 \pm 1.5$ and -30.9 ± 2.4 mV (with 10 μM retigabine); KCNQ2, $V_{1/2} = -38.8 \pm 0.8$ and -55.9 ± 0.6 mV (with 10 μM retigabine); KCNQ3, $V_{1/2} = -50.0 \pm 0.9$ and -89.4 ± 1.9 mV (with 10 μM retigabine). The shift of the I/I_{max} curve in response to 10 μM retigabine is strongest for KCNQ3 (−39.4 mV) (Fig. 1*E*) and intermediate for KCNQ2 (−17.1 mV) (Fig. 1*G*). In contrast, no statistically significant shift in $V_{1/2}$ could be observed for KCNQ1 (Fig. 1*F*), even at the highest retigabine concentration tested (100 μM) (Fig. 1*H*). These results agree well with the values reported from mammalian cells (Tatulian et al., 2001) and led us to construct chimeras between KCNQ1 and KCNQ3.

The shifts in the activation curves of KCNQ2 and KCNQ3 were clearly dependent on the concentration of retigabine (Fig.

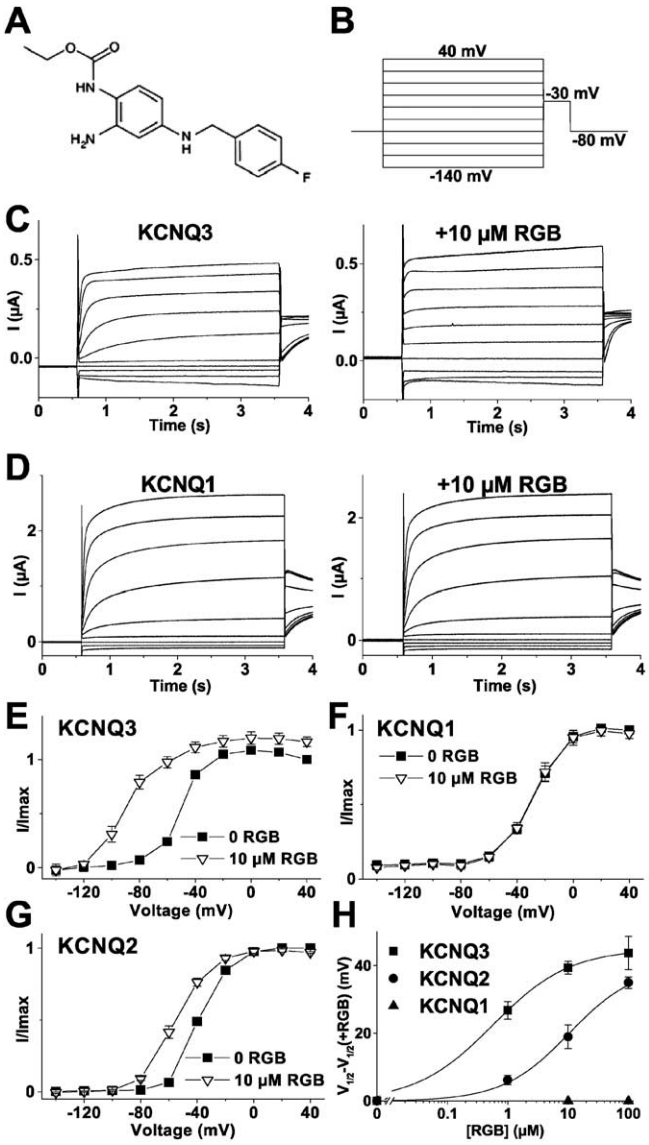

Figure 1. Retigabine sensitivities of KCNQ1 and KCNQ3. ***A***, Molecular structure of retigabine. ***B***, Voltage protocol used for the experiments shown in ***C–H***. From a holding potential of −80 mV, oocytes were clamped for 3 s to values between −140 and +40 mV, followed by a constant "tail" pulse of −30 mV. ***C***, ***D***, Effect of 10 μM retigabine (RBG) on currents from KCNQ3 (***C***) and KCNQ1 (***D***). Typical current traces recorded from *Xenopus* oocytes expressing KCNQ3 (***C***) and KCNQ1 (***D***) are shown. Currents before (***C***, ***D***, left) and after (***C***, ***D***, right) perfusion with 10 μM retigabine are displayed. ***E–G***, Voltage dependence of I/I_{max} curves of KCNQ3 (***E***), KCNQ1 (***F***), and KCNQ2 (***G***) measured in the absence or presence of 10 μM retigabine, obtained from tail current analysis as described in Materials and Methods. The voltage protocol is shown as in ***B***. ***H***, Retigabine dose–response curves for KCNQ1, KCNQ2, and KCNQ3. The relative shift values in voltage dependence were plotted against the retigabine concentration, and the data were fitted to the Hill equation.

1*H*). Fits of a Hill function to the data gave the following values: for KCNQ3, $K_{0.5} = 0.60 \pm 0.01$ μM, $n_H = 0.68 \pm 0.05$; KCNQ2, $K_{0.5} = 16.0 \pm 0.5$ μM, $n_H = 0.70 \pm 0.05$. In line with previous results (Tatulian et al., 2001) the values for the Hill coefficient n_H indicate that one retigabine molecule is sufficient to exert the activating effect on a single KCNQ2 or KCNQ3 channel.

Role of the ion-selective pore in retigabine sensitivity

Given the differential sensitivity of KCNQ3 and KCNQ1 to retigabine, we constructed chimeras between these proteins to identify structural determinants of retigabine activation. We aligned the transmembrane region of human KCNQ1 and KCNQ3 proteins with that of the bacterial K_v channel KvAP (Fig. 2*A*). Because the crystal structure of KvAP is known (Jiang et al., 2003), this alignment allows a more precise prediction of intramembrane helices of KCNQ channels, which was then used to guide the construction of chimeras. We first replaced the pore-lining segments (S5–S6) of KCNQ3 with the corresponding stretch of KCNQ1 and named this chimera KCNQ3(S5-P-S6;Q1) (Fig. 2*B*). It yielded currents that were >10-fold larger than KCNQ3 currents (Figs. 1*C*, 2*C*) and that were not changed by applying 10 μM retigabine (Fig. 2*C*), as judged from the invariant I/I_{max} or *I–V* curves (data not shown). This suggests that the segment encompassing helices S5–S6 and the pore region (P) are necessary for the retigabine sensitivity of KCNQ3. To transfer retigabine sensitivity into the KCNQ1 scaffold, we also constructed an inverse chimera [KCNQ1(S5-P-S6;Q3)], which, however, did not yield measurable currents.

Transfer of a stretch containing an N-glycosylation site from KCNQ1 boosts KCNQ3 expression

The pore region of KCNQ1 and KCNQ3 was divided into two parts. The extracellular "turret" domain (segment termed "TD") is poorly conserved between KCNQ1 and KCNQ3, whereas the inner pore part is highly homologous (Fig. 2*A*). We replaced either the TD segment or the whole pore region (Fig. 2*A*) of KCNQ3 by those of KCNQ1 in chimeras KCNQ3(TD;Q1) (Fig. 3*A*) and KCNQ3(P;Q1) (Fig. 3*C*), respectively. When expressed in *Xenopus* oocytes, both constructs gave large currents that were approximately 15- to 20-fold higher than those of KCNQ3 (Figs. 1*C*, 3*B*,*D*) and activated at voltages at approximately −60 mV. Their I/I_{max} curve decreased at voltages more positive than approximately +60 mV (Fig. 3*E*,*F*). Such a decrease in I/I_{max} was also observed for KCNQ1 and KCNQ3 (Fig. 1*F*,*E*, respectively) and might reflect an inactivation process at positive voltages (Tatulian et al., 2001).

The large increase in current amplitudes of these chimeras compared with those of KCNQ3 might be attributable to a larger single-channel conductance, an increased open probability, a larger number of active channels in the plasma membrane, or a combination of these factors. Nonstationary noise analysis was used to determine the single-channel conductance and maximal open probability of KCNQ3(TD;Q1) to 8.1 ± 0.7 pS and 0.65 ± 0.04, respectively (supplemental Fig. 1*A*, available at www.jneurosci.org as supplemental material). KCNQ3 was shown previously to have a conductance of 7.3 ± 0.7 pS and a maximal open probability of 0.42 ± 0.1 (Schwake et al., 2000). Thus, the increased current can be explained by neither an increase in single-channel conductance nor a changed open probability. After inserting hemagglutinin epitopes into extracellular parts of both channels, we determined their surface expression using a chemiluminescence assay (Zerangue et al., 1999; Schwake et al., 2000) (for methods and results, see supplemental information, available at www.jneurosci.org as supplemental material). The surface expression of KCNQ3HA(TD;Q1) was approximately fivefold increased compared with KCNQ3HA (supplemental Fig. 1*B*, available at www.jneurosci.org as supplemental material). Thus, the increase in surface expression, together with the slightly augmented maximal open probability, accounts for the large current amplitudes of KCNQ3(TD;Q1). In turn, the increased surface expression correlated with an overall increase of the expression level in Western blots (supplemental Fig. 1*C*, available at www.jneurosci.org as supplemental material). These blots also revealed an increase of the apparent molecular weight of

Table 1. $V_{1/2}$ values in absence or presence of retigabine for point mutations within the N-terminal part of S5 of KCNQ3(TD;Q1), KCNQ2–5 wild-type, and KCNQ1, KCNQ2, KCNQ4, and KCNQ5 tryptophan mutants

Mutation	$V_{1/2}$ (mV)	$V_{1/2}$ (mV;10 μM RGB)	$V_{1/2}$ (mV;100 μM RGB)	$\Delta V_{1/2}$ (mV;10 μM RGB)	$\Delta V_{1/2}$ (mV;100 μM RGB)
Q3-A253V	−13.3 ± 1.1	−48.4 ± 1.1		−35.1	
Q3-I254V	−38.2 ± 0.7	−63.4 ± 0.7		−25.2	
Q3-C255F	−41.7 ± 0.7	−78.4 ± 1.2		−36.7	
Q3-A256I	−13.1 ± 1.3	−38.6 ± 1.3		−25.5	
Q3-S258R	−56.5 ± 1.1	−97.4 ± 0.3		−40.9	
Q3-K259Q	2.7 ± 1.4	−31.3 ± 1.1		−34.0	
Q3-A264T	−0.5 ± 0.4	−31.5 ± 1.1		−31.0	
Q3-W265L	−73.6 ± 0.6	−73.3 ± 0.4	−73.1 ± 0.4	0.3	0.5
Q1 wild-type	−29.1 ± 1.5	−30.9 ± 2.4	−32.6 ± 2.5	−1.8	−3,5
Q2 wild-type	−38.8 ± 0.8	−55.9 ± 0.6	−75.5 ± 0.7	−17.1	−36.7
Q3 wild-type	−50.0 ± 0.9	−89.4 ± 1.9	−93.7 ± 4.9	−39.4	−43.7
Q4 wild-type	−11.7 ± 1.1	−16.3 ± 1.5	−36.5 ± 1.2	−4.6	−24.8
Q5 wild-type	−40.6 ± 0.8	−45.7 ± 1.3	−60.6 ± 1.2	−5.1	−20.0
Q2-W236L	−52.7 ± 0.6	−53.8 ± 0.7	−54.4 ± 0.7	−1.1	−1.7
Q4-W242L	−15.9 ± 1.8	−14.6 ± 1.9	−14.7 ± 1.8	+1.3	+1.2
Q5-W235L	−43.6 ± 1.3	−42.7 ± 1.4	−45.3 ± 1.3	0.9	−1.7
Q1-L266W	−45.3 ± 0.8	−49.4 ± 0.9	−53.2 ± 1.4	−4.1	−7.9

RGB, Retigabine.

KCNQ3(TD;Q1) compared with KCNQ3 (supplemental Fig. 1*C*, available at www.jneurosci.org as supplemental material). This suggests that the consensus sequence for N-glycosylation, which is present in the TD region of KCNQ1 but not in KCNQ3 (Fig. 2*A*), is used within the KCNQ3(TD;Q1) chimera. Indeed, disrupting the glycosylation consensus sequence by mutation of the asparagine (amino acid 288) (Fig. 2*A*) to alanine within the KCNQ3 (TD;Q1) chimera reduced the current to KCNQ3 wild-type level (data not shown). These results suggest that glycosylation of the channel leads to an increased expression level, possibly by increasing protein stability. This mechanism probably also applies to the KCNQ3(S5-P-S6;Q1) and KCNQ3(P;Q1) chimeras, because the currents measured for these constructs were increased, as well.

Role of the pore region in retigabine sensitivity

The replacement of either the total pore region [KCNQ3(P;Q1)] or of its N-terminal part [KCNQ3(TD;Q1)] by the corresponding segments of KCNQ1 (Fig. 3*A*,*C*) did not abolish their sensitivity to retigabine (Fig. 3*B*,*D*), which induced both an increase in current amplitude and a shift in voltage dependence. Activation parameters were as follows: KCNQ3(TD;Q1), $V_{1/2} = -28.2 \pm 1.4$ mV (without retigabine) and -73.7 ± 0.8 mV (with 10 μM retigabine); KCNQ3(P;Q1), $V_{1/2} = -36.8 \pm 1.2$ mV (without retigabine) and -54.2 ± 1.2 mV (with 10 μM retigabine). For these fits, values for KCNQ3(TD;Q1) at potentials more positive than +60 mV (without retigabine) or 0 mV (with retigabine) and for KCNQ3(P;Q1) values at potentials more positive than +40 mV (with retigabine) were excluded, because these are probably affected by a second (inactivation) gating process that leads to a decreased I/I_{max} curve at more positive potentials. However, the extent of the induced shift [−45.5 mV for KCNQ3(TD;Q1) and −17.4 mV for KCNQ3(P;Q1)] (Fig. 3*E*,*F*) differed between these chimeras. This difference is remarkable, because the two proteins differ in only six amino acids within the inner pore

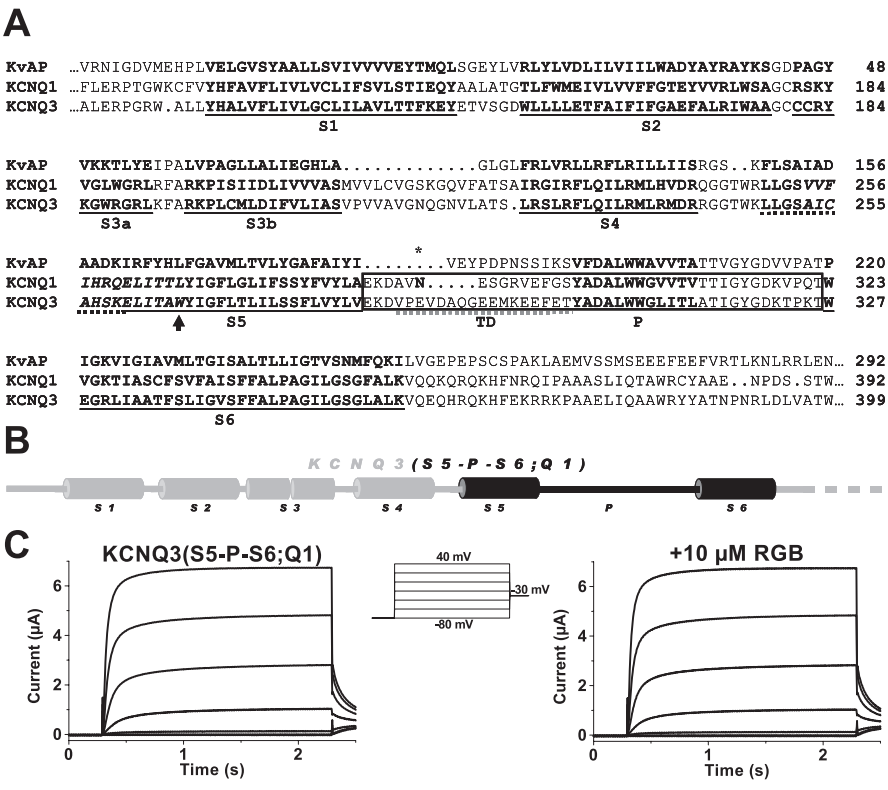

Figure 2. Sequence alignment of KvAP and human KCNQ1 and KCNQ3. ***A***, Sequence alignments of human KCNQ1, KCNQ3, and *Aeropyrum pernix* KvAP in the region encompassing the α-helices S1–S6 and the pore helix (P) are shown in bold and underlined, whereas the α-helical S4–S5 linker is underlined by a black dotted line. The pore regions, which consist of the extracellular turret domain (the TD segments underlined by a gray dotted line), pore helix, and selectivity filter of KCNQ1 and KCNQ3, are boxed. The S4–S5 linker and the N-terminal parts of S5 from KCNQ1 and KCNQ3 are shown in italics. The potential N-glycosylation site is indicated with an asterisk and the tryptophan residue with an arrow. ***B***, Schematic illustration of the chimera KCNQ3(S5-P-S6;Q1). ***C***, Current traces of the same oocyte expressing the chimera KCNQ3(S5-P-S6;Q1) before (left) and after (right) the application of 10 μM retigabine (RGB). The voltage protocol is shown in the inset in ***C***.

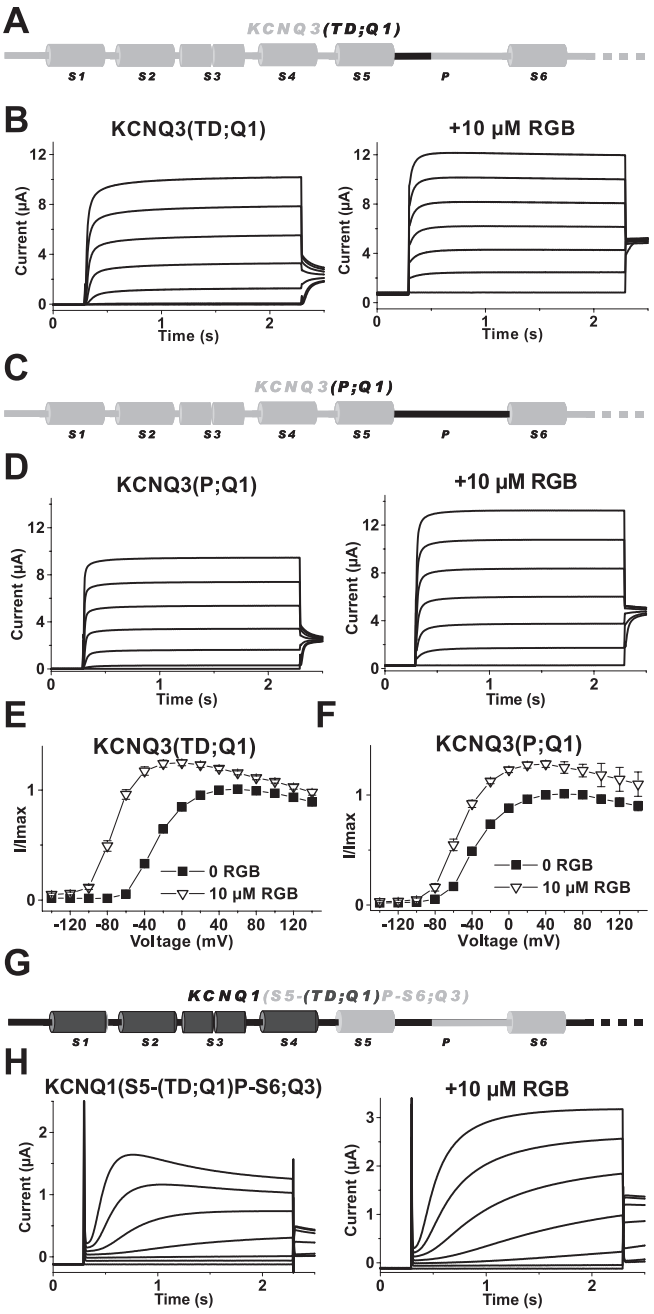

Figure 3. Retigabine sensitivities of KCNQ3(TD;Q1), KCNQ3(P;Q1), and KCNQ1(S5-(TD;Q1)P-S6;Q3). ***A***, ***C***, Schematic illustration of the chimeras KCNQ3(TD;Q1) (***A***) and KCNQ3(P;Q1) (***C***). ***B***, ***D***, Typical current traces of oocytes expressing the chimeras KCNQ3(TD;Q1) (***B***) and KCNQ3(P;Q1) (***D***) before and after the application of 10 μM retigabine (RGB). The voltage protocol used for these experiments is shown in the inset in Figure 2*C*. ***E***, ***F***, I/I_{max} curves of chimera KCNQ3(TD;Q1) (***E***) and chimera KCNQ3(P;Q1) (***F***) as a function of voltage obtained from tail current analysis. The voltage protocol corresponds basically to that shown in Figure 1*B*, but potentials from −140 to +140 mV were applied. The activation parameters as determined from fits of a Boltzmann function to I/I_{max} curves are stated in Results. ***G***, Schematic illustration of the chimera KCNQ1(S5-(TD;Q1)P-S6;Q3). ***H***, Typical current traces of the chimera KCNQ1(S5-(TD;Q1)P-S6;Q3) in response to a voltage protocol as in Figure 2*C* before and after the application of 10 μM retigabine.

vestibule (Fig. 2*A*) and suggests a modulatory role of the inner pore region on retigabine sensitivity. Because neither construct exhibited a loss of retigabine sensitivity, however, major determinants are likely to be present in S5 or S6 that were exchanged together with the pore region in the retigabine-insensitive KCNQ3(S5-P-S6;Q1) chimera (Fig. 2*C*).

Because the transfer of the TD segment from KCNQ1 into KCNQ3 did not abolish or reduce the sensitivity of the channel to retigabine, all additional chimeras included the TD fragment from KCNQ1 to boost their expression. This feature was used to increase the expression of KCNQ1(S5-P-S6;Q3), which did not yield measurable currents as described above. After insertion of the TD segment of KCNQ1, the resultant protein [KCNQ1(S5-(TD;Q1)-P-S6;Q3] (Fig. 3*G*) showed slowly activating currents (Fig. 3*H*). Importantly, these were strongly enhanced by retigabine (Fig. 3*H*). Thus, the exchange of the S5-P-S6 stretch between KCNQ1 and KCNQ3 qualitatively renders their sensitivity to this anticonvulsive drug. These results further confirmed our findings depicted in Figure 2 that the pore-lining segments (S5–S6) and the pore region (P) were responsible for retigabine sensitivity.

Role of the membrane-spanning segments S5 and S6 in retigabine sensitivity

To investigate the roles of the membrane segments S5 and S6 in retigabine sensitivity, we constructed a chimera termed KCNQ3(S5-TD;Q1), which contains the S5 segment and the current-enhancing TD part of KCNQ1 (Fig. 4*A*). It yielded slowly activating K^+ currents (Fig. 4B) that were essentially unaffected by retigabine, as revealed by the analysis of its tail currents (I/I_{max} curve; $V_{1/2} = -10.9 \pm 0.7$ mV without and -7 ± 0.6 mV with 10 μM retigabine) (Fig. 4*C*) and its invariant *I–V* curves (Fig. 4*D*).

In contrast, the KCNQ3(P-S6;Q1) chimera, in which the whole pore loop and the S6 segment from KCNQ1 were transferred into the KCNQ3 scaffold [KCNQ3(P-S6;Q1] (Fig. 4*E*), gave rise to large, fast-activating and retigabine-sensitive currents (Fig. 4*F*) whose voltage dependence was significantly shifted to hyperpolarizing voltages (Fig. 4*G*) ($V_{1/2} = -36.3 \pm 1.2$ mV without and -42 ± 1.1 mV with 10 μM retigabine), although the extent of this shift was less than that of the KCNQ3(P;Q1) chimera (Fig. 3*F*). As for other retigabine-sensitive KCNQ constructs and wild-type KCNQ3 (Fig. 1*E*), we observed an increase of the maximal I/I_{max} value at positive potentials (Fig. 4*G*). Retigabine increased also the stationary current amplitudes (Fig. 4*H*). Together with the retigabine insensitivity of the KCNQ3(S5-TD;Q1) chimera (Fig. 4*A–D*), these results suggested that the S5 rather than the S6 segment is responsible for the different retigabine sensitivity of KCNQ1 and KCNQ3.

Role of the N- and C-terminal parts of S5 in retigabine sensitivity

To narrow down the part of S5 that is important for retigabine sensitivity, we inserted an N-terminal part of S5 (pS5) into KCNQ3 (TD;Q1), resulting in the new chimera KCNQ3(pS5+TD;Q1) (Fig. 5*A*). The activation parameters for this construct were $V_{1/2} = 19.7 \pm 1.3$ mV (without retigabine) and 12.6 ± 1.1 mV (with 10 μM retigabine). However, the $V_{1/2}$ value in presence of retigabine determined by fitting a Boltzmann function to the data depended very much on the value of the normalized tail current amplitude at +60 mV, which exhibited a large error (Fig. 5*C*). If this value was excluded from the fit, a $V_{1/2}$ value of 16.9 ± 1.9 mV was obtained. Because the I/I_{max} values for the KCNQ3(pS5+TD;Q1) construct in the presence or absence of retigabine (and also the *I–V* curves) overlap within error limits (Fig. 5*C*,*D*), the shift in $V_{1/2}$ was regarded as insignificant, and this chimera is classified as insensitive to retigabine (Fig. 5*B–D*). Thus, the insertion of the N-terminal portion of S5 from KCNQ1 into the KCNQ3(TD;Q1) chimera is sufficient to abolish its reti-

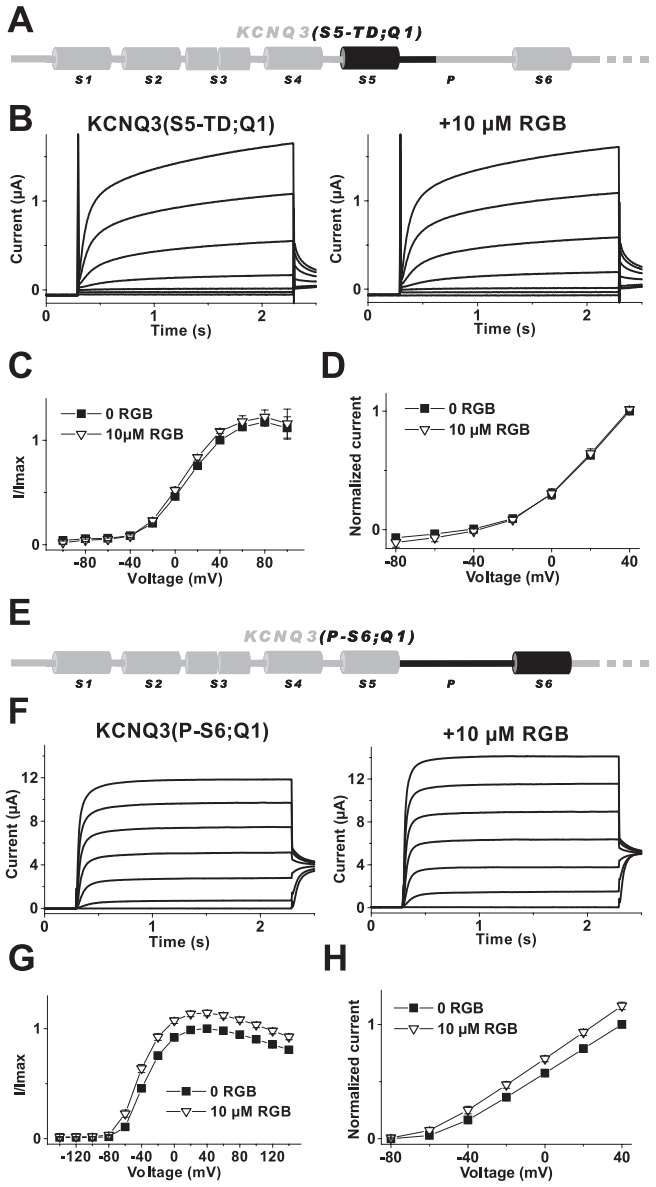

Figure 4. Retigabine sensitivities of KCNQ3(S5-TD;Q1) and KCNQ3(P-S6;Q1). ***A***, ***E***, Schematic illustration of the chimeras KCNQ3(S5-TD;Q1) (***A***) and KCNQ3(P-S6;Q1) (***E***). ***B***, ***F***, Typical current traces of the chimeras KCNQ3(S5-TD;Q1) (***B***) and KCNQ3(P-S6;Q1) (***F***) measured with a voltage protocol shown in the inset in Figure 2*C* before and after the application of 10 μM retigabine (RGB). ***C***, ***G***, I/I_{max} curves of chimera KCNQ3(S5-TD;Q1) (***A***) and chimera KCNQ3(P-S6;Q1) (***E***) as a function of voltage obtained from tail current analysis. [In the case of the chimera KCNQ3(S5-TD;Q1), cells were subjected to test pulses between −100 and 100 mV and for the chimera KCNQ3(P-S6;Q1) to test pulses between −140 and 140 mV (tail pulse voltage, −30 mV).] The activation parameters as determined from fits of a Boltzmann function to I/I_{max} curves are stated in Results. ***D***, ***H***, *I–V* curves of chimera KCNQ3(S5-TD;Q1) and chimera KCNQ3(P-S6;Q1) as a summary of the current recordings, which were obtained from oocytes measured with the voltage protocol shown in Figure 2*C*.

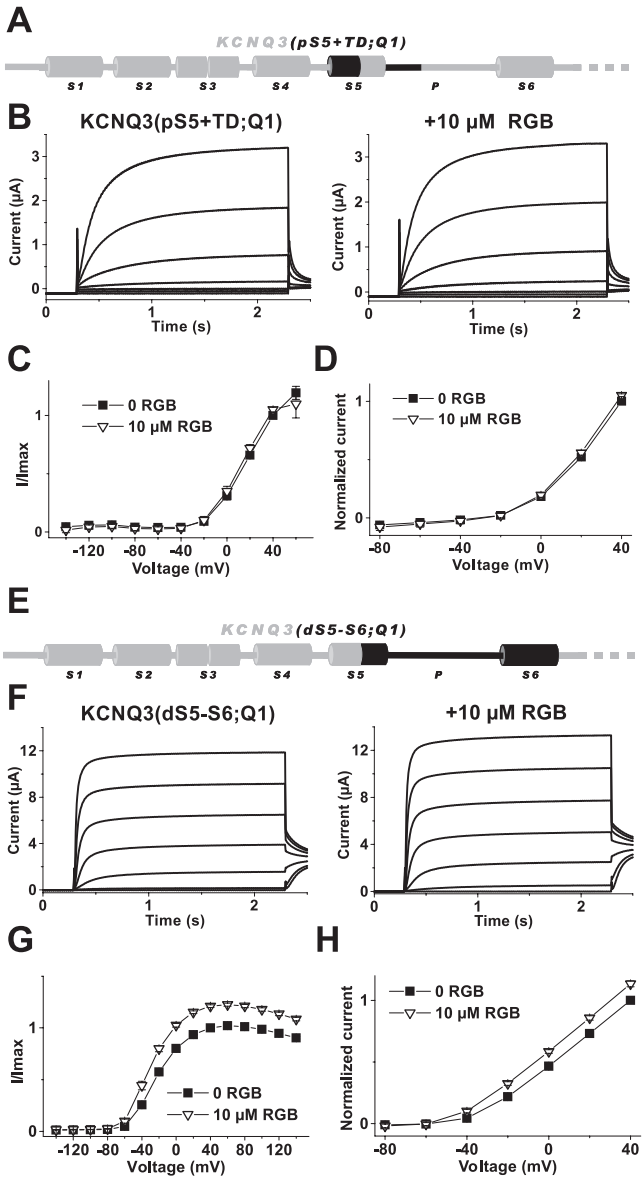

Figure 5. Retigabine sensitivities of KCNQ3(pS5+TD;Q1) and KCNQ3(dS5-S6;Q1). ***A***, ***E***, Schematic illustration of the chimeras KCNQ3(pS5+TD;Q1) (***A***) and KCNQ3(dS5-S6;Q1) (***E***). ***B***, ***F***, Typical current traces of the chimeras KCNQ3(pS5+TD;Q1) (***B***) and KCNQ3(dS5-S6;Q1) (***F***) measured with a voltage protocol shown in the inset in Figure 2*C* before and after the application of 10 μM retigabine (RGB). ***C***, ***G***, I/I_{max} curves of chimera KCNQ3(pS5+TD;Q1) (***A***) and chimera KCNQ3(dS5-S6;Q1) (***E***) as a function of voltage obtained from tail current analysis. [In the case of the chimera KCNQ3(pS5+TD;Q1), cells were subjected to test pulses between −140 and 60 mV and for the chimera KCNQ3(dS5-S6;Q1) to test pulses between −140 mV and 140 mV (tail pulse voltage, −30 mV).] The activation parameters as determined from fits of a Boltzmann function to I/I_{max} curves are stated in Results. ***D***, ***H***, *I–V* curves of chimera KCNQ3(pS5+TD;Q1) (***A***) and chimera KCNQ3(dS5-S6;Q1) (***E***) as a summary of the current recordings, which were obtained from oocytes measured with the voltage protocol shown in the inset in Figure 2*C*.

gabine sensitivity. Consequently, we next tested whether the insertion of the N-terminal part of S5 from KCNQ3 into the retigabine-insensitive KCNQ3(S5-P-S6;Q1) (Fig. 2*B*) could restore its drug sensitivity. The resulting construct [KCNQ3(dS5-S6;Q1)] (Fig. 5*E*) yielded currents that resembled those of KCNQ3(P-S6;Q1) chimera (Fig. 4*F*), both in terms of amplitude and moderate but significant retigabine sensitivity (activation parameters, $V_{1/2} = -22.9 \pm 1.2$ mV without and -29.8 ± 1.4 mV with 10 μM retigabine). The effect of retigabine was again ascertained by the analysis of I/I_{max} as a function of voltage (Fig. 5*G*) and by stationary current–voltage relationships (Fig. 5*H*). Together, the analysis of both chimeras (Fig. 5) strongly supports a role of the N-terminal part of S5 in conferring retigabine sensitivity to KCNQ3.

Identification of a critical residue in the N-terminal part of S5

The N-terminal halves of S5 from KCNQ1 and KCNQ3 differ in eight amino acids (Fig. 6*A*). Based on the well expressing KCNQ3(TD;Q1) construct, we generated point mutants in

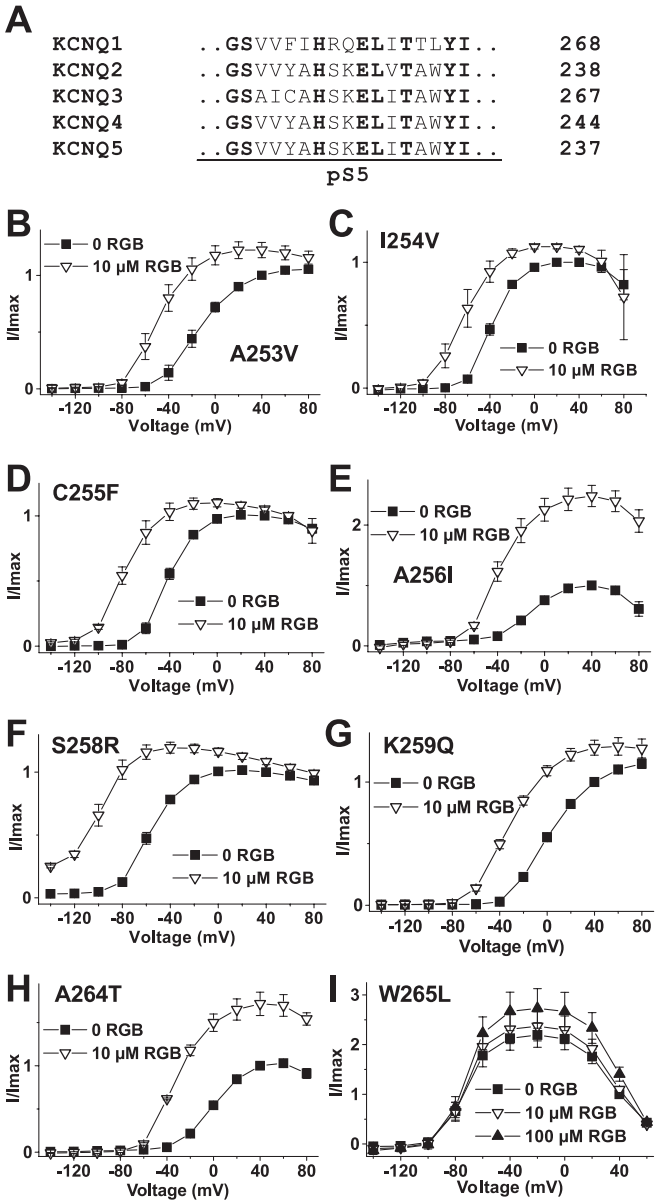

Figure 6. Retigabine (RGB) sensitivities of point mutations within the N-terminal part of S5 from KCNQ2 and KCNQ3. ***A***, Alignment of the N-terminal part of S5 forming amino acids from the KCNQ channels. ***B–I***, I/I_{max} curves of KCNQ3(TD;Q1)-A253V (***B***), KCNQ3(TD;Q1)-I254V (***C***), KCNQ3(TD;Q1)-C255F (***D***), KCNQ3(TD;Q1)-A256I (***E***), KCNQ3(TD;Q1)-S258R (***F***), KCNQ3(TD;Q1)-K259Q (***G***), KCNQ3(TD;Q1)-A264T (***H***), and KCNQ3(TD;Q1)-W265L (***I***) as a function of voltage obtained from tail current analysis. [In the case of the KCNQ3(TD;Q1) point mutations, cells were subjected to test pulses between −140 and 80 mV (tail pulse voltage, −30 mV).] The activation parameters are summarized in Table 1.

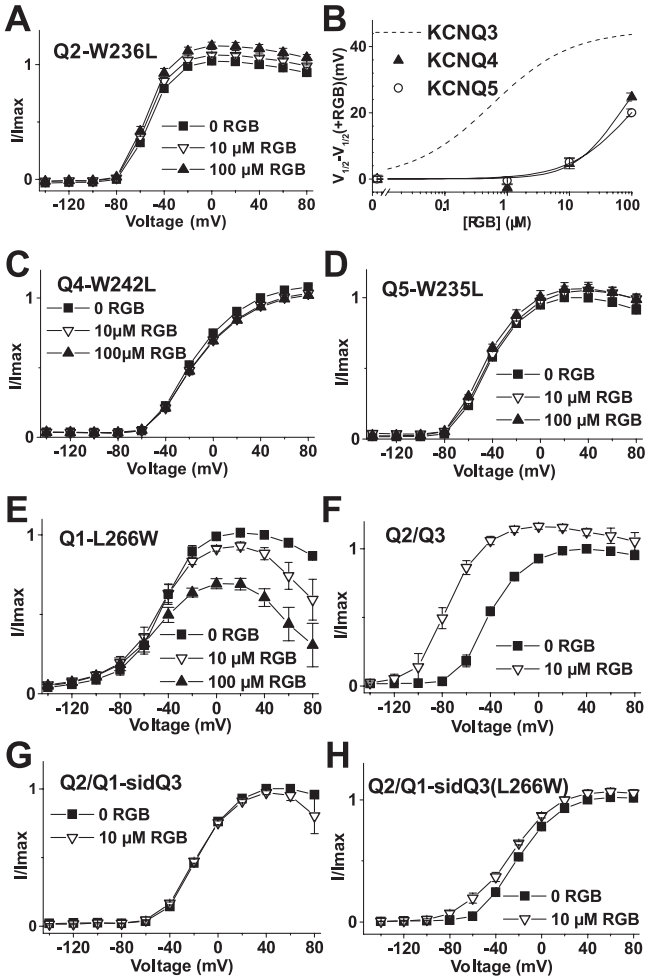

Figure 7. A single tryptophan is necessary for retigabine (RGB) sensitivity of KCNQ channels. The effect of retigabine on the I/I_{max} curves of KCNQ2-W236L (***A***), KCNQ4-W242L (***C***), KCNQ5-W235L (***D***), KCNQ1-L266W (***E***), KCNQ2/KCNQ3 (***F***), KCNQ1-sid_{Q3}/KCNQ2 (***G***), and KCNQ1(L266W)-sid_{Q3}/KCNQ2 (***H***) is shown. ***B***, Retigabine dose–response curves for KCNQ4 and KCNQ5. The relative shifts in $V_{1/2}$ values of the I/I_{max} curves were plotted against the retigabine concentration; the dose–response curve of KCNQ3 is depicted as a dashed line for comparison. Because for KCNQ4 and KCNQ5 no saturation of the retigabine-dependent shift in $V_{1/2}$ values was obtained at the highest retigabine concentration used, fits of a Hill function to the data were impossible. Solid lines in ***B*** were inserted to guide the eye.

which each of the KCNQ3 residues was individually replaced by the corresponding amino acid of KCNQ1 and investigated their I/I_{max} curves as a function of voltage (Fig. 6*B–I*). Most mutations changed this voltage dependence (Fig. 6*B–I*; Table 1). Compared with KCNQ3(TD;Q1), mutations of four residues (A253V, A256I, K259Q, and A264T) shifted the half-maximal voltage of activation $V_{1/2}$ to depolarizing potentials, whereas the remaining four mutants (I254V, C255F, S258R, and W265L) displayed a hyperpolarizing shift. This effect was particularly pronounced for mutation S258R. Application of 10 μM retigabine shifted the $V_{1/2}$ values of all but one construct by more than −20 mV (Fig. 6*B–I*; Table 1). The single exception was mutant W265L, which displayed a very small, insignificant $V_{1/2}$ shift (0.3 mV) during addition of 10 μM retigabine. To rule out the possibility, that just the dose–response curve of the mutant KCNQ3 channel is different, higher concentrations of retigabine were applied to oocytes expressing the KCNQ3(TD;Q1)-W265L channel construct. Even during addition of 100 μM retigabine, the $V_{1/2}$ shift was insignificant (0.5 mV). These experiments identified tryptophan-265 as being necessary for the retigabine sensitivity of KCNQ3.

A single tryptophan is necessary for retigabine sensitivity of KCNQ channels

The tryptophan residue in KCNQ3 identified thus far is conserved between KCNQ2 and KCNQ5 (Fig. 6*A*), all of which are retigabine sensitive (Tatulian et al., 2001; Wickenden et al., 2001) and expressed in neurons (Jentsch, 2000). We therefore asked whether mutation of the equivalent tryptophan in KCNQ2, KCNQ4, and KCNQ5 to leucine would abolish their retigabine sensitivity, as well. As for KCNQ3 (Fig. 1*E*,*H*) or KCNQ2 (Fig. 1*G*,*H*), I/I_{max} curves of both KCNQ4 and KCNQ5 (Fig. 7*B*) were shifted during addition of retigabine in a dose-dependent man-

ner ($V_{1/2}$ values listed in Table 1). In contrast, shifts in $V_{1/2}$ of the I/I_{max} curves in response to 10 μM retigabine for the tryptophan mutants KCNQ2-W236L (Fig. 7*A*) [$V_{1/2}$ (shift) = −1.1 mV], KCNQ4-W242L (Fig. 7*C*) [$V_{1/2}$ (shift) = 1.3 mV], and KCNQ5-W235L (Fig. 7*D*) [$V_{1/2}$ (shift) = 0.9 mV] are abolished within error limits, which holds true for even higher concentrations of this compound (see $V_{1/2}$ values in Table 1). These results are in line with the loss of retigabine sensitivity of KCNQ3(TD;Q1)-W265L (Fig. 6*I*), although in the latter case, still a slight increase of the maximal I/I_{max} values at more positive potentials than −40 mV was observed at high retigabine concentrations.

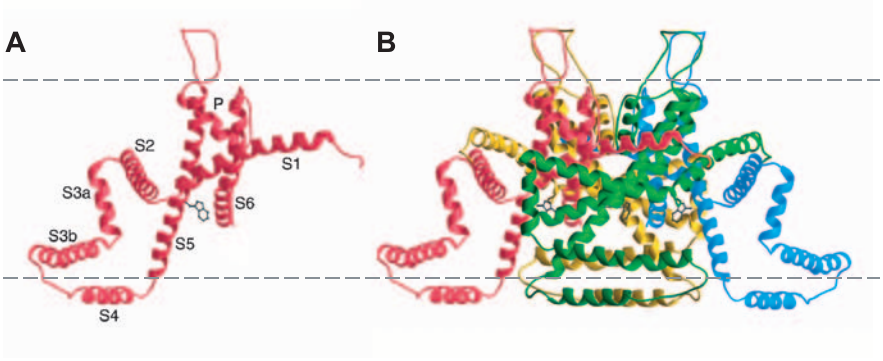

Figure 8. Structural model of KCNQ3. Ribbon representation of a single KCNQ3 subunit (***A***) and the tetrameric KCNQ3 channel (***B***), according to model building as described in Materials and Methods. The extracellular side of the protein is facing up, and the dashed lines outline the approximate boundaries of the membrane. Helical elements are numerically labeled for the transmembrane segments (S1–S6) and the pore helix (P) (***A***). The tryptophan residue critical for retigabine activation of KCNQ3 is shown as a ball-and-stick representation in gray within the S5 segment.

Whereas exchanging the crucial S5 tryptophan for leucine in KCNQ2–KCNQ5 leads to loss of retigabine sensitivity, a replacement of the corresponding leucine by a tryptophan in KCNQ1 (mutant KCNQ1-L266W) rendered KCNQ1 sensitive to this anticonvulsant. However, the effect of the compound in this case was more complex, because, for the KCNQ1-L266W mutant, a concentration-dependent reduction in current amplitudes (data not shown) and a decrease of the maximal I/I_{max} values at more positive potentials than −20 mV was observed in addition to a small but dose-dependent shift of the activation parameters ($V_{1/2}$ = −45.3 ± 0.8 mV without retigabine, −49.4 ± 0.9 mV with 10 μM retigabine, and −53.2 ± 1.4 mV with 100 μM retigabine) (Fig. 7*E*). These results indicate that the introduction of the tryptophan residue into KCNQ1 in this position confers some gain in retigabine sensitivity, although this effect is not as clear-cut as the loss in sensitivity for the Trp-to-Leu mutants of KCNQ2–KCNQ5. Therefore, a tryptophan at this position is considered as necessary, but not sufficient, for the complete retigabine sensitivity of KCNQ channels, because the effect of retigabine on the KCNQ1-L266W mutant was clearly different compared with KCNQ2–KCNQ5.

Retigabine sensitivity of heteromeric KCNQ2/KCNQ3 and KCNQ1-*sid*$_{Q3}$/KCNQ2 channels

The fact that KCNQ channels are tetramers raised the question of how many subunits need to have a tryptophan in S5 to confer retigabine sensitivity to the channel. We addressed this issue by analyzing heteromeric KCNQ channels assembled from retigabine-sensitive KCNQ2 subunits and retigabine-insensitive constructs containing the KCNQ1 transmembrane domains. Because KCNQ1 wild-type does not assemble with KCNQ2, we used a chimera termed KCNQ1-*sid*$_{Q3}$ that contains the C-terminal subunit interaction domain (*sid*) from KCNQ3. This construct forms heteromeric channels with KCNQ2 in a similar manner as KCNQ3 (Schwake et al., 2003). Most important for this study, a KCNQ1-*sid*$_{Q3}$ construct carrying the mutation G314S exerted a dominant-negative effect on KCNQ2 currents, indicating that a common pore is formed by these two subunits. Whereas KCNQ3/KCNQ2 channels were retigabine-sensitive [$V_{1/2}$ (shift) = −33.9 mV] (Fig. 7*F*), KCNQ1-*sid*$_{Q3}$/KCNQ2 heteromeric channels showed no activation by retigabine (Fig. 7*G*). This result was surprising because coexpression of two subunits will cause a mixture of homomeric channels and heteromeric channels with different subunit stoichiometries. At least homomeric KCNQ2 channels in this mixture should have produced, albeit to a low extent, a shift in the voltage dependence of activation. However, the theoretically to-be-expected low amount of homomeric KCNQ2 channels of 6.25% (assuming random assembly of subunits) and the fact that currents mediated by KCNQ1-*sid*$_{Q3}$/KCNQ2 heteromeric channels are approximately eightfold larger than KCNQ2-mediated currents (Schwake et al., 2003) can account for the observed lack of retigabine sensitivity in a KCNQ1-*sid*$_{Q3}$/KCNQ2 heteromeric expression situation.

Assuming a 2:2 stoichiometry, these results suggested that the two S5 tryptophan residues present, on average, within the KCNQ1-*sid*$_{Q3}$/KCNQ2 tetramers are not sufficient for activation by retigabine. To ensure that four equivalent S5 tryptophans would confer retigabine sensitivity in the framework of this heteromeric channel, we coexpressed a KCNQ1(L266W)-*sid*$_{Q3}$ chimera with KCNQ2 and assayed the effect of retigabine (Fig. 7*H*). Heteromeric KCNQ1(L266W)-*sid*$_{Q3}$/KCNQ2 channels exhibited significant retigabine sensitivity [$V_{1/2}$ (shift) = −7.5 mV]. Although this effect was less pronounced than for KCNQ2/KCNQ3 channels (Fig. 7*F*,*H*), it underlines the importance of the tryptophan residue for mediating retigabine sensitivity also within KCNQ heteromers.

Predicted location of the crucial tryptophan residue in the KCNQ3 channel

Based on the crystal structure of a voltage-gated potassium channel from *Aeropyrum pernix* KvAP (Jiang et al., 2003), we constructed a three-dimensional model (Fig. 8*A*,*B*) for the S1–S6 membrane region of KCNQ3 (see Materials and Methods), which was based on the sequence alignment shown in Figure 2*A*. There is still debate about the arrangement of the voltage sensor-forming membrane segments S1–S4 in the KvAP structure (Swartz, 2004). However, the ion conduction pore is very similar to that of the KcsA (Doyle et al., 1998) and the MthK channel (Jiang et al., 2002), which only contain the pore-forming segments without a voltage sensor. A comparison between these regions in the closed KcsA and the open MthK channel indicates that the S6 gate is open in KvAP and that in all cases the adjacent inner (S6) and outer (S5) helices of each subunit maintain an approximately antiparallel relationship to each other (Doyle et al., 1998; Jiang et al., 2002, 2003). These features probably also apply for eukaryotic voltage-gated potassium channels, such as KCNQ3. The tryptophan residue in KCNQ3 is located at the interface between S5 and S6 within each subunit (Fig. 8*A*). According to our model, these segments form a hydrophobic groove

to which S1 from another subunit might contribute. This groove might be part of the hydrophobic retigabine binding pocket.

Discussion

KCNQ potassium channels are of great physiological and medical importance. They are promising targets for the development of drugs for indications such as epilepsy or chronic pain (Jentsch, 2000). The targeting of neuronal KCNQ channels should avoid adverse effects on KCNQ1, because an interference with the activity of that channel could compromise cardiac function, as demonstrated by human inherited diseases (Wang et al., 1996; Neyroud et al., 1997; Chen et al., 2003). One promising compound known to activate KCNQ2–KCNQ5 channels with differential potencies is the anticonvulsant retigabine (Tatulian et al., 2001). It is known to exert its effect by shifting the voltage dependence of activation and increasing the maximal open probability (Tatulian and Brown, 2003). The molecular mechanism of this interaction, however, remained elusive so far.

In the present experiments, we provide evidence that a single amino acid, a tryptophan within the central part of the S5 segment, is critical for the retigabine sensitivity of KCNQ2–KCNQ5. This tryptophan has been identified by analyzing chimeras between KCNQ1 and KCNQ3, using the differential sensitivity of these isoforms toward retigabine (Tatulian et al., 2001). Mutation of this crucial residue dramatically reduced the retigabine sensitivity of KCNQ3 [investigated with the construct KCNQ3(TD;Q1) that shows enhanced current levels]. Because a tryptophan at this position is found in all retigabine-sensitive KCNQ channels but is not present at the equivalent position in the retigabine-insensitive KCNQ1, we mutated also the equivalent Trp of KCNQ2, KCNQ4, and KCNQ5 to Leu. As observed for KCNQ3, also the mutants KCNQ2(W236L), KCNQ4(W242L), and KCNQ5(W235L) exhibited a loss of retigabine sensitivity. However, the introduction of a tryptophan at this position in KCNQ1 led to a slight retigabine sensitivity of the resulting KCNQ1(L266W) construct, although it has to be noted that, in addition, other properties of channel activation were changed, which might indicate that still other residues can contribute to drug binding. Our results suggest that the tryptophan residue forms a critical part of the retigabine binding site in KCNQ channels. Its location in transmembrane helix S5 suggests that retigabine does not bind directly in the ion-conducting pathway.

According to our KCNQ3 model, the tryptophan residue is located at the interface between S5 (outer helix) and S6 (inner helix), near the intracellular gate of the channel. Structure-based mechanistic models of the gating process in voltage-dependent potassium channels assume that the voltage sensor, which is attached directly to the outer helix by the S4–S5 linker, might open the pore by pulling the outer helix away from the central pore axis, causing the inner helices to follow (Jiang et al., 2003). It is tempting to speculate that retigabine exerts its action by interfering with this process, thereby shifting the voltage sensitivity of the KCNQ2–KCNQ5 channels in the hyperpolarizing direction.

The model predicts one retigabine binding site per subunit and that binding of retigabine does not interfere with the ion-conductive pore (Fig. 8). It has been reported that the action of retigabine at strongly positive potentials appeared to be complicated by a secondary inhibitory action (Main et al., 2000; Tatulian et al., 2001), which was most clearly seen with KCNQ1 channels, but probably extends to KCNQ2 and KCNQ2/3. Because KCNQ1 is affected, it is unlikely that this secondary inhibitory effect of retigabine relies on the same interaction site.

Tatulian et al. (2001) reported a Hill constant of ~1 from dose–response curves measured for KCNQ2/3, KCNQ2, KCNQ3, and KCNQ4, which suggests a noncooperative process (Tatulian et al., 2001). However, because each subunit within a tetramer carries its own retigabine binding site, the activating effect of the drug could be an all-or-none phenomenon, implying that all four sites must be occupied for the conformational change to occur. In keeping with this proposal, coexpression of KCNQ2 with KCNQ1-sid_{Q3} led to a retigabine-insensitive current. Because a mixture of KCNQ2/KCNQ1-sid_{Q3} heteromers with different stoichiometries probably mediates this current, it is likely that one retigabine-insensitive KCNQ1-derived subunit within the heterotetramer is sufficient to interfere with the sensitivity of the channel to retigabine. This conclusion is supported by the fact that KCNQ1(L266W)-sid_{Q3}/KCNQ2 heteromers are retigabine sensitive. Thus, four tryptophan residues within a heterotetramer seem to be necessary for activation of KCNQ channels by retigabine. The reduced sensitivity of KCNQ1(L266W)-sid_{Q3}/KCNQ2 compared with KCNQ2/KCNQ3 heteromers can be attributable to modulating effects of additional amino acids, which differ between KCNQ1 and KCNQ3.

The expression of KCNQ3 was boosted by inserting the extracellular turret domain (termed TD segment) from KCNQ1 into KCNQ3. We believe that the strongly augmented KCNQ3(TD;Q1) currents are attributable to N-linked glycosylation. This, in turn, leads to an increased protein level, possibly by increasing protein stability or a more efficient trafficking of the channel. It has been shown that N-glycosylation affects the stability and trafficking of members of the K_v1 subfamily and might constitute a common mechanism to promote the trafficking of voltage-gated potassium channels to the cell surface (Watanabe et al., 2004).

Recently, an alanine at position 315 in the inner pore vestibule of KCNQ3 was identified that exerts a strong negative effect on current flow (Etxeberria et al., 2004). The authors speculate that this residue shapes a binding site for a putative endogenous blocking molecule (Etxeberria et al., 2004). Because the chimeras KCNQ3(TD;Q1) (carrying the A315 of KCNQ3) and KCNQ3(P;Q1) (not carrying the alanine in equivalent position) gave rise to comparable current amplitudes (Fig. 3*B*,*D*), it might be possible that the turret domain of KCNQ3 contributes to the binding pocket. Alternatively, glycosylation could prevent the binding of the putative blocking particle. Additional experiments are needed to investigate the role of the pore region in trafficking and stability of the KCNQ3 protein or to prove the blocking particle hypothesis.

After submission of this work, a paper was published (Wuttke et al., 2005), in which the key role of the tryptophan in S5 was also highlighted. In addition, also the conserved residue Gly-301 in KCNQ2, which is considered to be the gating hinge, was suggested to be involved in conferring retigabine sensitivity. In contrast to the KCNQ1/KCNQ3 chimeras investigated in the present study, these authors used chimeras (in combination with single amino acid substitutions) between KCNQ1 and KCNQ2 for narrowing down the interaction site for the drug. Whereas replacement of the KCNQ2 tryptophan by the homologous amino acid of KCNQ1 in the KCNQ2(W236L) construct abolished retigabine sensitivity, involvement of the Gly-301 residue could not be directly shown, because the KCNQ2(G301A) construct was not functional. However, participation of S6 residues in mediating the retigabine effect could be inferred during complete replacement of S6 in the KCNQ1(S6)Q2 construct, although the retigabine effect was somewhat different, resulting in a −7.4 mV shift of the activation curve and a threefold current increase. In accordance with the results presented here, transfer of the residues

Trp-236 and Gly-301 from KCNQ2 into homologous positions within the KCNQ1 scaffold was not sufficient to render KCNQ1 retigabine sensitive, no matter whether the residues were exchanged singly or in tandem. Finally, Wuttke and coworkers constructed a chimera termed KCNQ2(S6)Q1, in which the KCNQ1 S6 segment was inserted into the KCNQ2 scaffold. This construct was retigabine insensitive, as expected, but back-mutating the gating hinge residue within the KCNQ2(S6)Q1[A336G] construct again conferred retigabine sensitivity, as judged from a −13 mV shift and a dose-dependent increase in currents. However, the authors did not investigate the number of retigabine-sensitive subunits within a tetramer, because no heteromeric KCNQ expression studies were undertaken. The experiments performed by Wuttke et al. further strengthen the findings of this study, and the same conclusions are reached, most importantly concerning the role of the S5 tryptophan. Retigabine interferes with the activation gate of the channel, in effect stabilizing the open-channel conformation.

In summary, we conclude that the presence of a tryptophan residue within the central part of the S5 segment of KCNQ2–KCNQ5 is necessary but not completely sufficient for the effect of retigabine and suggest that this side chain is a major structural element of the retigabine binding site.

References

Biervert C, Schroeder BC, Kubisch C, Berkovic SF, Propping P, Jentsch TJ, Steinlein OK (1998) A potassium channel mutation in neonatal human epilepsy. Science 279:403–406.

Brown DA, Adams PR (1980) Muscarinic suppression of a novel voltage-sensitive K^+ current in a vertebrate neurone. Nature 283:673–676.

Carson M (1991) RIBBONS 2.0. J Appl Cryst 24:958–961.

Charlier C, Singh NA, Ryan SG, Lewis TB, Reus BE, Leach RJ, Leppert M (1998) A pore mutation in a novel KQT-like potassium channel gene in an idiopathic epilepsy family. Nat Genet 18:53–55.

Chen YH, Xu SJ, Bendahhou S, Wang XL, Wang Y, Xu WY, Jin HW, Sun H, Su XY, Zhuang QN, Yang YQ, Li YB, Liu Y, Xu HJ, Li XF, Ma N, Mou CP, Chen Z, Barhanin J, Huang W (2003) KCNQ1 gain-of-function mutation in familial atrial fibrillation. Science 299:251–254.

Cooper EC, Aldape KD, Abosch A, Barbaro NM, Berger MS, Peacock WS, Jan YN, Jan LY (2000) Colocalization and coassembly of two human brain M-type potassium channel subunits that are mutated in epilepsy. Proc Natl Acad Sci USA 97:4914–4919.

Doyle DA, Morais Cabral J, Pfuetzner RA, Kuo A, Gulbis JM, Cohen SL, Chait BT, MacKinnon R (1998) The structure of the potassium channel: molecular basis of K^+ conduction and selectivity. Science 280:69–77.

Etxeberria A, Santana-Castro I, Regalado MP, Aivar P, Villarroel A (2004) Three mechanisms underlie KCNQ2/3 heteromeric potassium M-channel potentiation. J Neurosci 24:9146–9152.

Gutman GA, Chandy KG, Adelman JP, Aiyar J, Bayliss DA, Clapham DE, Covarriubias M, Desir GV, Furuichi K, Ganetzky B, Garcia ML, Grissmer S, Jan LY, Karschin A, Kim D, Kuperschmidt S, Kurachi Y, Lazdunski M, Lesage F, Lester HA, et al. (2003) International Union of Pharmacology. XLI. Compendium of voltage-gated ion channels: potassium channels. Pharmacol Rev 55:583–586.

Jentsch TJ (2000) Neuronal KCNQ potassium channels: physiology and role in disease. Nat Rev Neurosci 1:21–30.

Jiang Y, Lee A, Chen J, Cadene M, Chait BT, MacKinnon R (2002) Crystal structure and mechanism of a calcium-gated potassium channel. Nature 417:515–522.

Jiang Y, Lee A, Chen J, Ruta V, Cadene M, Chait BT, MacKinnon R (2003) X-ray structure of a voltage-dependent K^+ channel. Nature 423:33–41.

Kubisch C, Schroeder BC, Friedrich T, Lutjohann B, El-Amraoui A, Marlin S, Petit C, Jentsch TJ (1999) KCNQ4, a novel potassium channel expressed in sensory outer hair cells, is mutated in dominant deafness. Cell 96:437–446.

Main MJ, Cryan JE, Dupere JR, Cox B, Clare JJ, Burbidge SA (2000) Modulation of KCNQ2/3 potassium channels by the novel anticonvulsant retigabine. Mol Pharmacol 58:253–262.

Neyroud N, Tesson F, Denjoy I, Leibovici M, Donger C, Barhanin J, Faure S, Gary F, Coumel P, Petit C, Schwartz K, Guicheney P (1997) A novel mutation in the potassium channel gene KVLQT1 causes the Jervell and Lange-Nielsen cardioauditory syndrome. Nat Genet 15:186–189.

Schroeder BC, Kubisch C, Stein V, Jentsch TJ (1998) Moderate loss of function of cyclic-AMP-modulated KCNQ2/KCNQ3 K^+ channels causes epilepsy. Nature 396:687–690.

Schroeder BC, Hechenberger M, Weinreich F, Kubisch C, Jentsch TJ (2000) KCNQ5, a novel potassium channel broadly expressed in brain, mediates M-type currents. J Biol Chem 275:24089–24095.

Schwake M, Pusch M, Kharkovets T, Jentsch TJ (2000) Surface expression and single channel properties of KCNQ2/KCNQ3, M-type K^+ channels involved in epilepsy. J Biol Chem 275:13343–13348.

Schwake M, Jentsch TJ, Friedrich T (2003) A carboxy-terminal domain determines the subunit specificity of KCNQ K^+ channel assembly. EMBO Rep 4:76–81.

Singh NA, Charlier C, Stauffer D, DuPont BR, Leach RJ, Melis R, Ronen GM, Bjerre I, Quattlebaum T, Murphy JV, McHarg ML, Gagnon D, Rosales TO, Peiffer A, Anderson VE, Leppert M (1998) A novel potassium channel gene, KCNQ2, is mutated in an inherited epilepsy of newborns. Nat Genet 18:25–29.

Swartz KJ (2004) Towards a structural view of gating in potassium channels. Nat Rev Neurosci 5:905–916.

Tatulian L, Brown DA (2003) Effect of the KCNQ potassium channel opener retigabine on single KCNQ2/3 channels expressed in CHO cells. J Physiol (Lond) 549:57–63.

Tatulian L, Delmas P, Abogadie FC, Brown DA (2001) Activation of expressed KCNQ potassium currents and native neuronal M-type potassium currents by the anti-convulsant drug retigabine. J Neurosci 21:5535–5545.

van Gunsteren WF, Billeter SR, Eising AA, Hühnenberger PH, Krüger P, Mark AE, Scott WRP, Tironi IG (1996) Biomolecular simulation: the GROMOS 96 manual and user guide. Zurich: vdf Hochschul-Verlag.

Vriend G (1990) WHAT IF: a molecular modeling and drug design program. J Mol Graph 8:52–56, 29.

Wang HS, Pan Z, Shi W, Brown BS, Wymore RS, Cohen IS, Dixon JE, McKinnon D (1998) KCNQ2 and KCNQ3 potassium channel subunits: molecular correlates of the M-channel. Science 282:1890–1893.

Wang Q, Curran ME, Splawski I, Burn TC, Millholland JM, VanRaay TJ, Shen J, Timothy KW, Vincent GM, de Jager T, Schwartz PJ, Toubin JA, Moss AJ, Atkinson DL, Landes GM, Connors TD, Keating MT (1996) Positional cloning of a novel potassium channel gene: KVLQT1 mutations cause cardiac arrhythmias. Nat Genet 12:17–23.

Watanabe I, Zhu J, Recio-Pinto E, Thornhill WB (2004) Glycosylation affects the protein stability and cell surface expression of Kv1.4 but not Kv1.1 potassium channels. A pore region determinant dictates the effect of glycosylation on trafficking. J Biol Chem 279:8879–8885.

Wickenden AD, Yu W, Zou A, Jegla T, Wagoner PK (2000) Retigabine, a novel anti-convulsant, enhances activation of KCNQ2/Q3 potassium channels. Mol Pharmacol 58:591–600.

Wickenden AD, Zou A, Wagoner PK, Jegla T (2001) Characterization of KCNQ5/Q3 potassium channels expressed in mammalian cells. Br J Pharmacol 132:381–384.

Wuttke TV, Seebohm G, Bail S, Maljevic S, Lerche H (2005) The new anticonvulsant Retigabine favors voltage-dependent opening of the Kv7.2 (KCNQ2) channel by binding to its activation gate. Mol Pharmacol 67:1009–1017.

Yang WP, Levesque PC, Little WA, Conder ML, Ramakrishnan P, Neubauer MG, Blanar MA (1998) Functional expression of two KvLQT1-related potassium channels responsible for an inherited idiopathic epilepsy. J Biol Chem 273:19419–19423.

Zerangue N, Schwappach B, Jan YN, Jan LY (1999) A new ER trafficking signal regulates the subunit stoichiometry of plasma membrane K(ATP) channels. Neuron 22:537–548.